Vietnam Journal of Marine Science and Technology; Vol. 20, No. 2; 2020: 231–243
DOI: https://doi.org/10.15625/1859-3097/20/2/15066
http://www.vjs.ac.vn/index.php/jmst

Research on the stability of the 3D frame on coral foundation subjected to impact load

Nguyen Thanh Hung[1,*], Nguyen Thai Chung[2], Hoang Xuan Luong[2]

[1]*University of Transport Technology, Hanoi, Vietnam*
[2]*Department of Solid Mechanics, Le Quy Don Technical University, Hanoi, Vietnam*
[*]E-mail: hungnt@utt.edu.vn

Received: 19 March 2019; Accepted: 30 September 2019

Abstract
This article presents an application of the finite element method (FEM) for the stability analysis of 3D frame (space bar system) on the coral foundation impacted by collision impulse. One-way joints between the rod and the coral foundation are described by the contact element. Numerical analysis shows the effect of some factors on the stability of the bar system on coral foundation. The results of this study can be used for stability analysis of the bar system on coral foundation subjected to sea wave load.

Keywords: Stability, 3D beam element, slip element, coral foundation.

Citation: Nguyen Thanh Hung, Nguyen Thai Chung, Hoang Xuan Luong, 2020. Research on the stability of the 3D frame on coral foundation subjected to impact load. *Vietnam Journal of Marine Science and Technology*, *20*(2), 231–243.

INTRODUCTION

Most of the structures built on the coral foundation are frames that consist of 3D beam elements. Under the wave and wind loading, response of the structure is periodical. However, in the case of strong waves and wind or ships approaching, the structural system is usually subjected to impact load. The simultaneous impact of horizontal and vertical loads may lead the structure to instability. So, the stability calculation of the 3D beam structure on coral foundation is necessary. Nguyen Thai Chung, Hoang Xuan Luong, Pham Tien Dat and Le Tan [1, 2] used 2D slip element and finite element method for dynamic analysis of single pile and pipe in the coral foundation in the Spratly Islands. Mahmood and Ahmed [3], Ayman [4] studied nonlinear dynamic response of 3D-framed structures including soil structure interaction effects. Hoang Xuan Luong, Nguyen Thai Chung and other authors [5, 6] have systematically studied physical properties of corals of Spratly Islands and obtained a number of results on interaction between structures and coral foundation on these islands. Graham and Nash [7] assessed the complexity of the coral shelf structure by studying the published literature. Therefore, the interaction between the structures and coral foundation is an important problem in dynamic analysis of offshore structures that was basically considered in [8, 9]. In addition, the vertical static load may significantly affect the stability of a structure when the impact is applied horizontally. Therefore, study of the factors mentioned above is important and this is the subject of the present work. Thus, in this paper, an algorithm is proposed for evaluating stability of the frame structure on coral foundation under static load P_d and horizontal impact load P_N that allows one to find the critical forces in different cases.

GOVERNING EQUATIONS AND FINITE ELEMENT FORMULATION

The 3D beam element formulation of the frame

Using the finite element method, the frame is simulated by three dimensional 2-node beam elements with 6 degrees of freedom per node (fig. 1).

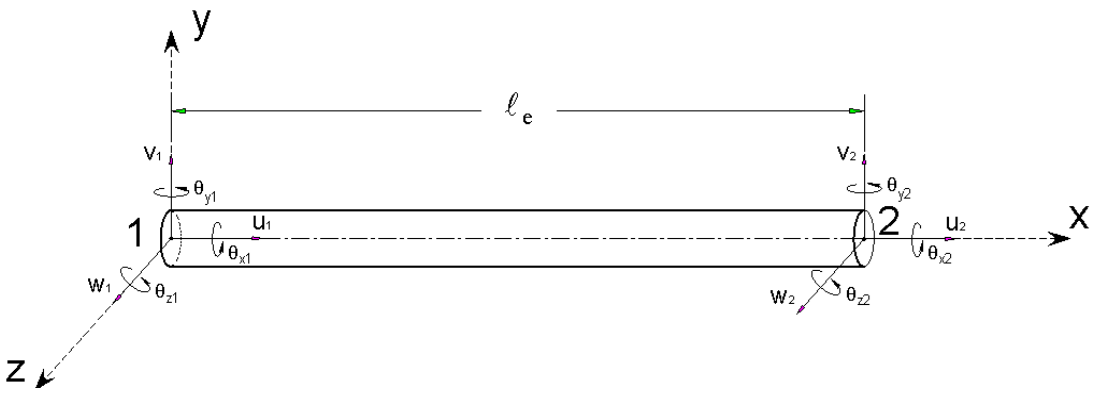

Figure 1. Three dimensions 2-node beam element model

Displacement at any point in the element [10, 13]:

$$\begin{aligned} u &= u\ x,y,z,t\ = u_0\ x,t\ + z\theta_y\ x,t\ - y\theta_z\ x,t\ , \\ v &= v\ x,y,z,t\ = v_0\ x,t\ - z\theta_x\ x,t\ , \\ w &= w\ x,y,z,t\ = w_0\ x,t\ + y\theta_x\ x,t \end{aligned} \tag{1}$$

Where: t represents time; *u*, *v* and *w* are displacements along *x, y* and *z*; θ_x is the rotation of cross-section about the longitudinal axis *x*, and θ_x, θ_z denote rotation of the cross-section

about y and z axes; the displacements with subscript "0" represent those on the middle plane ($y = 0$, $z = 0$).

The strain components are [10, 12]:

$$\begin{aligned}\varepsilon_x &= \frac{\partial u}{\partial x}+\frac{1}{2}\left(\frac{\partial v}{\partial x}\right)^2+\frac{1}{2}\left(\frac{\partial w}{\partial x}\right)^2=\frac{\partial u_0}{\partial x}+z\frac{\partial \theta_y}{\partial x}-y\frac{\partial \theta_z}{\partial x}+\frac{1}{2}\left(\frac{\partial v_0}{\partial x}-z\frac{\partial \theta_x}{\partial x}\right)^2+\frac{1}{2}\left(\frac{\partial w_0}{\partial x}-y\frac{\partial \theta_x}{\partial x}\right)^2\\ &=\frac{\partial u_0}{\partial x}+z\frac{\partial \theta_y}{\partial x}-y\frac{\partial \theta_z}{\partial x}+\frac{1}{2}\left(\left(\frac{\partial v_0}{\partial x}\right)^2+\left(\frac{\partial w_0}{\partial x}\right)^2+\left(\frac{\partial \theta_x}{\partial x}\right)^2\left(y^2+z^2\right)\right),\\ \gamma_{zx} &= \frac{\partial u}{\partial z}+\frac{\partial w}{\partial x}=\frac{\partial w_0}{\partial x}+y\frac{\partial \theta_x}{\partial x}+\theta_y,\\ \gamma_{xy} &= \frac{\partial u}{\partial y}+\frac{\partial v}{\partial x}=\frac{\partial v_0}{\partial x}-z\frac{\partial \theta_x}{\partial x}-\theta_z\end{aligned} \tag{2}$$

The latter equations can be rewritten in the vector form:

$$\{\varepsilon\}=\{\varepsilon\}^L+\{\varepsilon\}^{NL} \tag{3}$$

In which: $\{\varepsilon\}^L, \{\varepsilon\}^{NL}$ are linear and non-linear strain vectors, respectively.

The constitutive equation can be written as:

$$\{\sigma\}=\begin{Bmatrix}\sigma_x\\ \tau_{zx}\\ \tau_{xy}\end{Bmatrix}=\begin{bmatrix}E & 0 & 0\\ 0 & G & 0\\ 0 & 0 & G\end{bmatrix}\begin{Bmatrix}\varepsilon_x\\ \gamma_{zx}\\ \gamma_{xy}\end{Bmatrix}=[D]\{\varepsilon\}=[D]\left\{\varepsilon^L\right\}+[D]\left\{\varepsilon^{NL}\right\} \tag{4}$$

Where: $[D]=\begin{bmatrix}E & 0 & 0\\ 0 & G & 0\\ 0 & 0 & G\end{bmatrix}$ is the matrix of material constants, E is the elastic modulus of longitudinal deformation, G is the shear modulus.

Nodal displacement vector for the beam element is defined as:

$$\{q\}_e=\left\{u_1 \;\; v_1 \;\; w_1 \;\; \theta_{x_1} \;\; \theta_{y_1} \;\; \theta_{z_1} \;\; u_2 \;\; v_2 \;\; w_2 \;\; \theta_{x_2} \;\; \theta_{y_2} \;\; \theta_{z_2}\right\}^T \tag{5}$$

Dynamic equations of 3D element can be derived by using Hamilton's principle [11, 13]:

$$\delta\int_{t_1}^{t_2}\left[T_e-U_e+W_e\right]dt=0 \tag{6}$$

Where: T_e, U_e, W_e are the kinetic energy, strain energy, and work done by the applied forces of the element, respectively.

The kinetic energy at the element level is defined as:

$$T^e=\frac{1}{2}\int_{V_e}\rho\{\dot{u}\}^T\{\dot{u}\}\,dV \tag{7}$$

Where: V_e is the volume of the plate element, $\{u\}=[N]\{q\}_e$ is the vector of displacements, $[N]$ is the matrix of shape functions.

The strain energy can be written as:

$$U^e=\frac{1}{2}\int_{V_e}\{\varepsilon\}^T\{\sigma\}\,dV \tag{8}$$

The work done by the external forces:

$$W^e=\int_{V_e}\{u\}^T\{f_b\}\,dV+\int_{S_e}\{u\}^T\{f_s\}\,dS+\{u\}^T\{f_c\} \tag{9}$$

In which: $\{f_b\}$ is the body force, S_e is the surface area of the plate element, $\{f_s\}$ is the surface force, and $\{f_c\}$ is the concentrated load. Substituting equations (3), (4) into (8) and then substituting (7), (8), (9) into (6), the dynamic equation for the beam element is obtained in the form:

$$\left[M\right]_e^b \{\ddot{q}\}_e + \left(\left[K\right]_e^b + \left[K_G\right]_e^b\right)\{q\}_e = \{f\}_e^b \quad (10)$$

Where: $\left[K\right]_e^b$ is the linear stiffness matrix, given in Appendix A.1, $\left[K_G\right]_e^b$ is the non-linear stiffness matrix (geometric matrix), given in Appendix A.2, $\left[M\right]_e^b$ is the mass matrix, given in Appendix A.3 [13], [15], and $\{f\}_e^b$ is the nodal force vector.

Finite element formulation of coral foundation

The coral foundation is simulated by 8-node solid elements with 3 degrees of freedom per node (fig. 2).

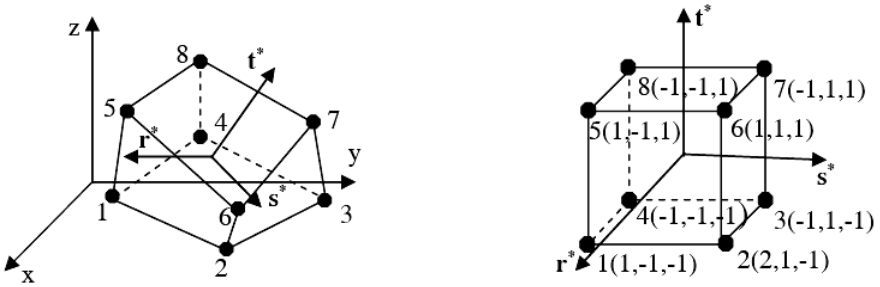

a) In the global coordinate system b) In the local coordinate system

Figure 2. 8-node solid element

The element stiffness and mass matrices are defined as [12, 13]:

$$\left[K\right]_e^s = \int_{V_e} \left[B\right]_s^T \left[D\right]_s \left[B\right]_s dV \quad (11)$$

$$\left[M\right]_e^s = \int_{V_e} \rho_s \left[N\right]_s^T \left[N\right]_s dV \quad (12)$$

The dynamic equation of the element can be written as [11, 13]:

$$\left[M\right]_e^s \{\ddot{q}\}_e + \left[K\right]_e^s \{q\}_e = \{f\}_e^s \quad (13)$$

In which: $[B]_s$ is relation matrix between deformation - strain and $[D]_s$ - elastic constant matrix of 8-node solid element, ρ_s is the density of soil, $[N]_s$ is the shape function matrix.

The 3D slip element linking the beam element and coral foundation

To characterize the contact between the beams surface and coral foundation (can be compressive, non-tensile [5, 6, 15]), the authors used three-dimensional slip elements (3D slip elements). This type of element has very small thickness, used for formulation of the contact layer between the beams and the coral foundation, the geometric modeling of the element is shown in fig. 3.

The stiffness matrix of the slip element in the local coordinates is [16, 17]:

$$\left[K\right]_e^{slip} = \iint \left[N\right]^T \left[k\right] \left[N\right] dxdy \quad (14)$$

Where:

$$\left[N\right] = \left[-B_1 \;\; -B_2 \;\; -B_3 \;\; -B_4 \;\; B_1 \;\; B_2 \;\; B_3 \;\; B_4\right] \quad (15)$$

Matrix $[B_i]$ contains the interpolation functions of the element and is given by:

$$\left[B_i\right]=\begin{bmatrix} h_i & 0 & 0 \\ 0 & h_i & 0 \\ 0 & 0 & h_i \end{bmatrix},\ h_i=\frac{1}{4}\left(1\pm\xi_i\right)\left(1\pm\eta_i\right) \tag{16}$$

and [*k*] is the material property matrix containing unit shear and normal stiffness, which is defined as:

$$\left[k\right]=\begin{bmatrix} k_{sx} & 0 & 0 \\ 0 & k_{sy} & 0 \\ 0 & 0 & k_{nz} \end{bmatrix} \tag{17}$$

Where: k_{sx}, k_{sy} denote unit shear stiffness along *x* and *y* directions, respectively; and k_{nz} denotes unit normal stiffness along the *z* direction, they are defined in table 1.

In table 1, *v* is the Poisson's ratio, *E* is the longitudinal elasticity modulus, and G_{res} is the transversal elasticity modulus of the coral foundation.

It should be noted that due to the special contact of beams and coral foundation as described above, in the slip elements, the stiffness matrix, $\left[K\right]_e^{slip}$ is dependent on displacement vector $\left\{q\right\}_e$ [1, 17]:

$$\left[K\right]_e^{slip}=\left[K\left(\left\{q\right\}_e\right)\right]_e^{slip}$$

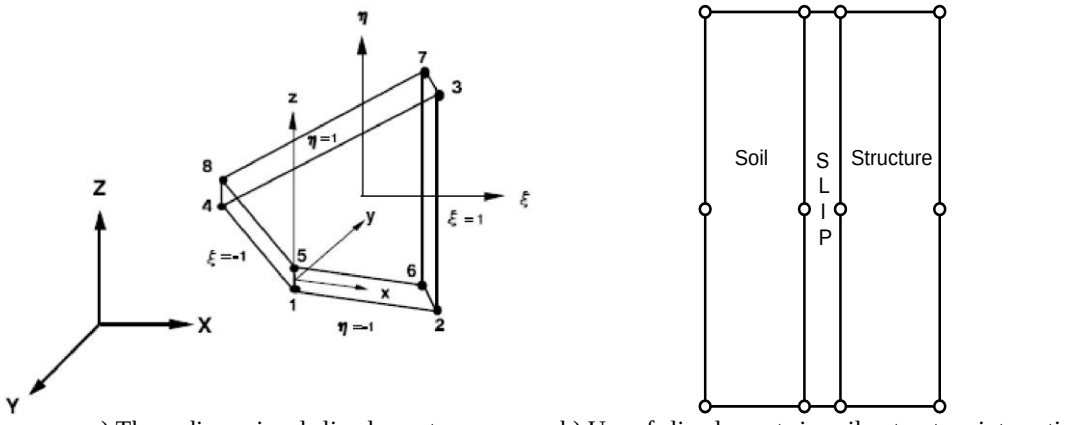

a) Three-dimensional slip element b) Use of slip elements in soil - structure interaction

Figure 3. Three-dimensional slip element and use of the element

Table 1. Material property matrix

k_{nz}	Force/(Length)^2	$k_{nz}=\frac{E(1-\nu)}{(1+\nu)(1-2\nu)}$
k_{sx}, k_{sy}	Force/(Length)^2	$k_{sx}=k_{sy}=\frac{E}{2(1+\nu)}$
k_{res}	Force/(Length)^2	$k_{res}=G_{res}$

Equation of motion of the system and algorithm for solution

By assembling all element matrices and nodal force vectors, the governing equations of motions of the total system can be written as:

$$\left[M\right]\{\ddot{q}\}+\left(\left[K\right]+\left[K_G\right]\right)\{q\}=\{f\} \tag{18}$$

Where:

$$[M]=\sum_{N_e^b+N_e^s}\left([M]_e^b+[M]_e^s\right),[K]=\sum_{N_e^b+N_e^s+N_e^{slip}}\left([K]_e^b+[K]_e^s+[K]_e^{slip}\right)=\left[K\left(\{q\}\right)\right],$$
$$\left[K_G\right]=\sum_{N_e^b}\left[K_G\right]_e^b,\{f\}=\sum_{N_e^b+N_e^s}\left(\{f\}_e^b+\{f\}_e^s\right) \quad (19)$$

and N_e^b, N_e^s, N_e^{slip} are the numbers of beam, solid and slip elements, respectively.

In case of consideration of damping force $\{f_d\}=-[C]\{q\}$, the dynamic equation of the system becomes:

$$[M]\{\ddot{q}\}+[C]\{\dot{q}\}+\left(\left[K\left(\{q\}\right)\right]+\left[K_G\right]\right)\{q\}=\{f\} \quad (20)$$

Where: $[C]=\alpha[M]+\beta\left([K]+\left[K_G\right]\right)=\left[C\left(\{q\}\right)\right]$ is the overall structural damping matrix, and α, β are Rayleigh damping coefficients [11, 14].

The non-linear equation (20) is solved by using the Newmark method for direct integration and Newton-Raphson method in iteration processes. A computation program is established in Matlab environment, which includes the loading vector updated after each step:

Step 1. Defining the matrices, the external load vector, and errors of load iterations.

Step 2. Solving the equation (20) to present a load vector.

Step 3. Checking the following stability conditions.

If the displacement of the frame does not increase over time: define stress vector, update the geometric stiffness matrices [K_G] and [K]. Increase load, recalculate from step 2;

If the displacement of the frame increases over time, the system is buckling: *Critical load* $p = p_{cr}$, $t = t_{cr}$. End.

RESULTS AND DISCUSSION

Basic problem

Let's consider the system shown in fig. 4 which has structural parameters as follows: Dimensions H_1 = 8.5 m, H_2 = 22.2 m, H_3 = 24.0 m, H_4 = 5 m, B_1 = 16 m, B_2 = 25 m, corner of main pile β = 8°. The main piles, horizontal bar and the oblique bar have the annular cross-section, in which outer diameter of main piles D_{ch} = 0,8 m, thickness of piles t_{ch} = 3.0 cm; outer diameter of horizontal bar and the oblique bar D_{th} = 0.4 m, thickness of piles t_{th} = 2.0 cm. The cross-section of bars connecting main piles at height (H_1 + H_2 + H_3) is of *I* shape with size: width b_I = 0.4 m, height h_I = 1.0 m, web thickness th_g = 0.04 m. Frame is made of steel, with material parameters: Young modulus E = 2.1×10^{11} N/m^2, Poisson's coefficient ν = 0.3, density ρ = 7850 kg/m^3, depth of pile in the coral foundation H_0 = 10 m (fig. 4a).

Foundation parameters: The coral foundation contains four layers; the physicochemical characteristics of the substrate layers are derived from experiments performed on Spratly Islands as shown in table 2.

With the error in iteration of study ε_{tt} = 0.5, after the iteration, the size of coral foundation is defined as: $B_N = L_N$ = 80 m, H_N = 20 m.

Boundary conditions: Clamped supported on the bottom, simply supported on four sides and free at the top of the research domain.

Load effects: The vertical static load P_d at the top of 4 main piles of the system is $P_d = 10^6$ N, the impact load at the top of 2 main piles in the horizontal direction x: $P_N = P(t)$ has ruled as shown in fig. 4b, where $P_0 = 10^6$ N, $\Delta\tau$ = 0.5 s.

Table 2. Characteristics of coral foundation layer's materials [1–3]

Layer	Depth (m)	E_f (N/cm^2)	ν_f	ρ_f (kg/m^3)	Friction coefficient with steel f_{ms}	Damping coefficient ξ
1	2	2.83×10^4	0.22	2.55×10^3	0.21	0.05
2	10	2.19×10^5	0.25	2.60×10^3	0.32	

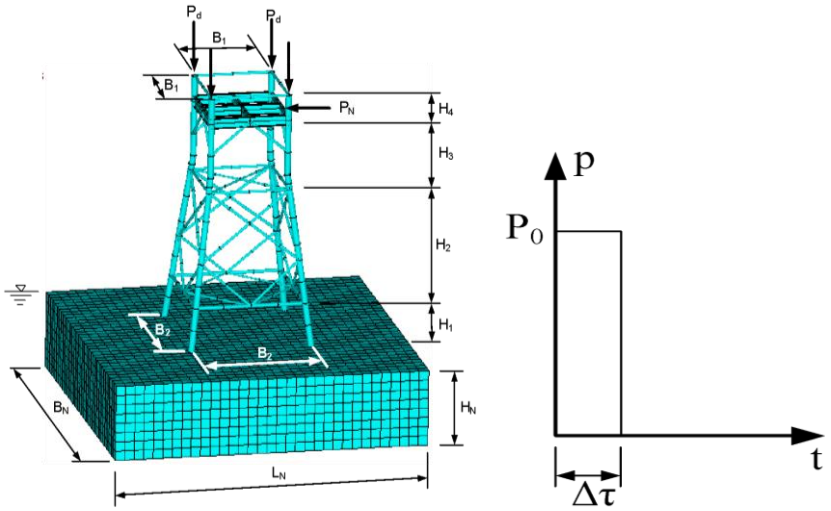

a) Computational model b) Impact load law

Figure 4. Computational model and impact load law

Vertical and horizontal displacement and acceleration response (according to the direction of collision) at the top of the bar system are shown in figs. 5–8 and table 3.

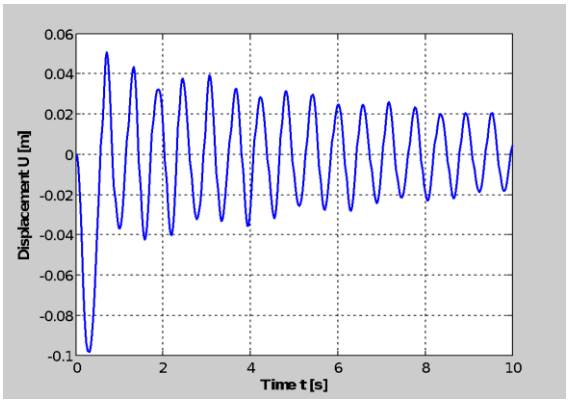

Figure 5. Displacement u at the top of the frame

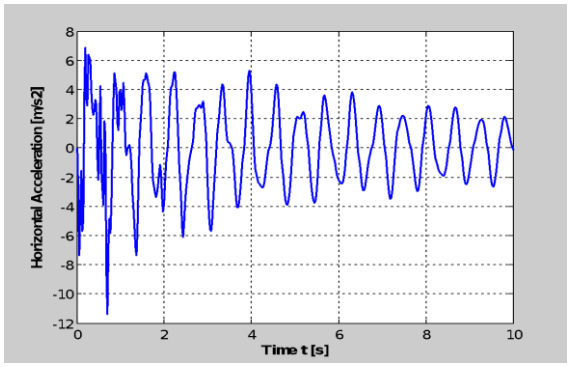

Figure 7. Horizontal acceleration at the top of the frame

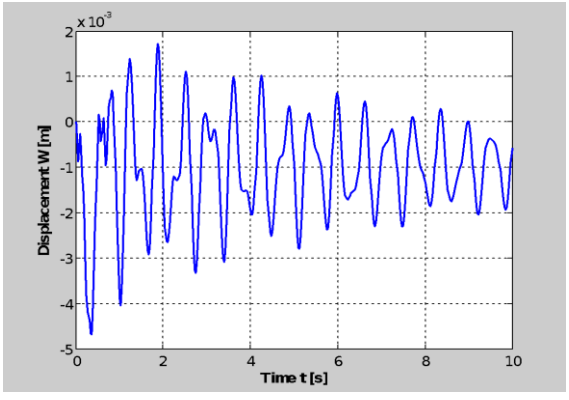

Figure 6. Displacement w at the top of the frame

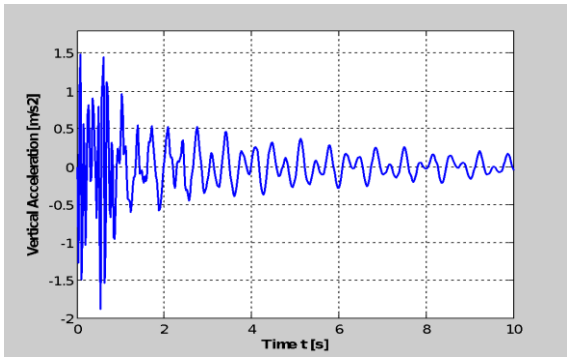

Figure 8. Vertical acceleration at the top of the frame

Comment: Under action of a horizontal pulse, displacement and acceleration response at the top of the system will have the sudden change. After the impact has finished, the response will gradually return to the stable stage. For horizontal response, the stable point comes to 0, while for vertical response, stable displacement value differs from 0 because the static load on the system still exists.

Table 3. Displacement response at the top of the bar system

	u_{max} (m)	w_{max} (m)	$\ddot{u}_{max}$ (m/s^2)	$\ddot{w}_{max}$ (m/s^2)
Value	0.0984	0.00469	11.399	1.885

Effect of horizontal impact on the stability of the system

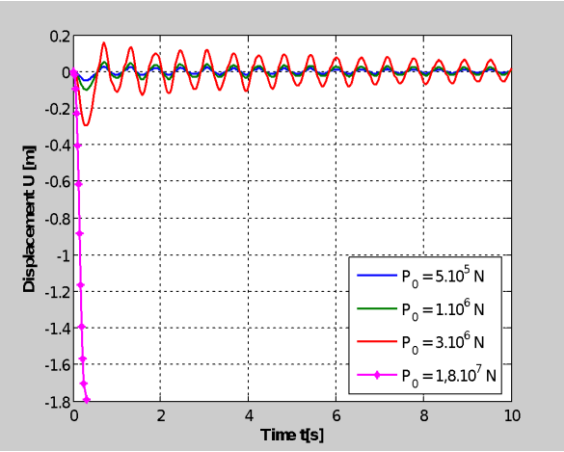

Figure 9. Displacement u at the top of the frame

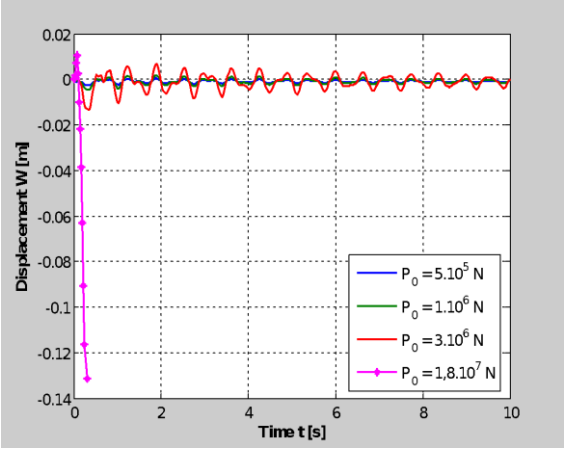

Figure 10. Displacement w at the top of the frame

To evaluate the effect of horizontal impulse on the stability of the beam system with the same values of the structural parameters of the problem, we only increase the value P_0 of horizontal impulse. Responses at the calculated points are shown in figs. 9–12 and table 4.

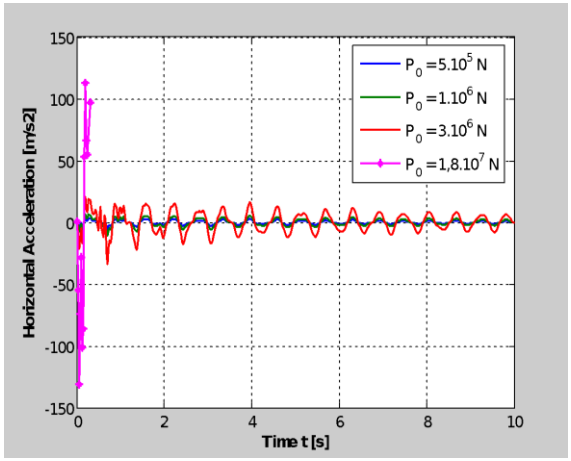

Figure 11. Horizontal acceleration at the top of the frame

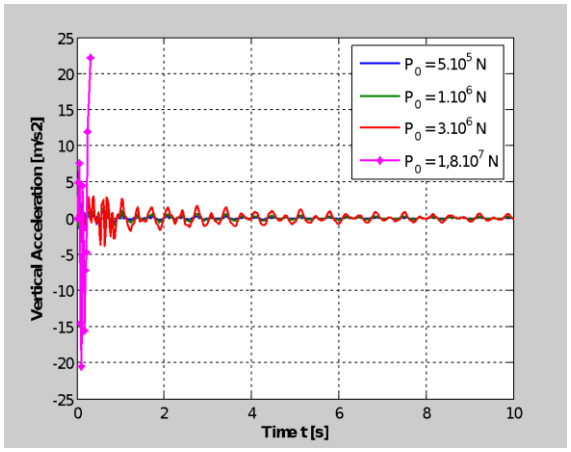

Figure 12. Vertical acceleration at the top of the frame

Comment: When impulse P_0 increases, the extreme response at the points of calculation increases. This extreme value jumps when $P_0 = 1.8\times10^7$ N, at this time the computer program only runs a few steps and then stops, does not run out of computational time as in previous cases. In this case, the system is unstable.

Table 4. Transition and acceleration response at the top of the system according to the P_0

P_0 [N]	U_{max} [m]	W_{max} [m]	$\ddot{U}_{max}$ [m/s^2]	$\ddot{W}_{max}$ [m/s^2]
5×10^5	0.0492	0.00277	5.697	1.905
1×10^6	0.0984	0.00469	11.399	1.885
3×10^6	0.2954	0.0136	34.144	3.845
1.8×10^7	1.7924	0.1312	131.253	22.219

Effect of static load on the stability of the system

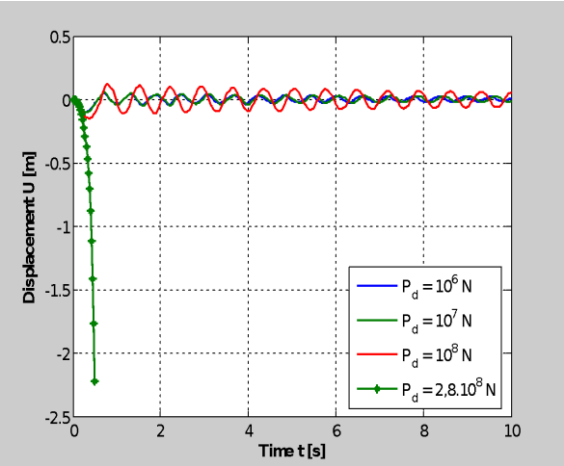

Figure13. Displacement *u* at the top of the frame

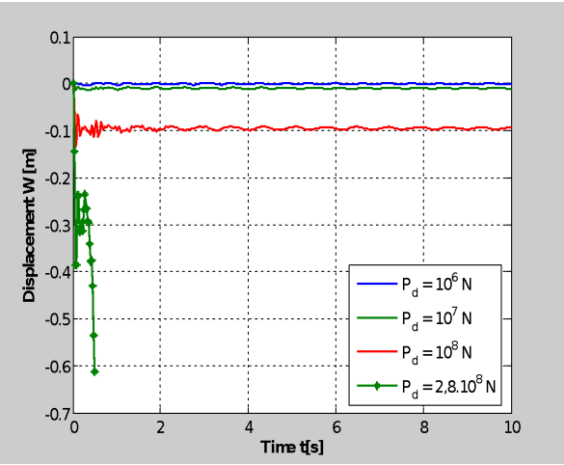

Figure 14. Displacement *w* at the top of the frame

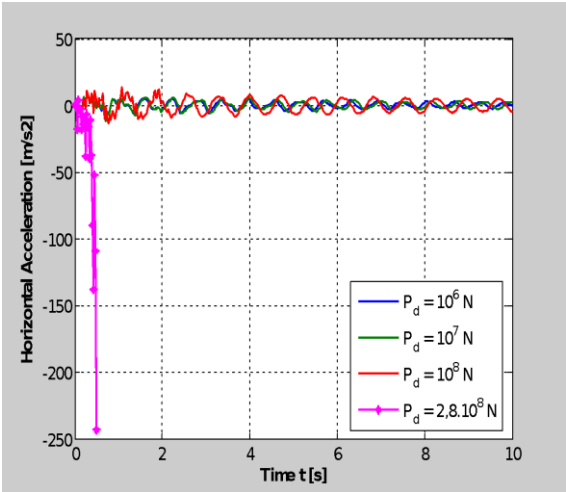

Figure 15. Horizontal acceleration at the top of the frame

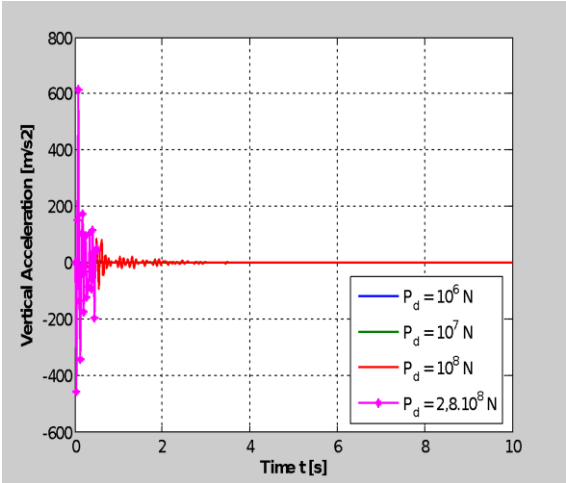

Figure 16. Vertical acceleration at the top of the frame

To evaluate the effect of static load on the stability of the bar system and find the critical value of the static load while keeping the impulse $P_0 = 10^6$ N, the authors increase the value of the force P_d, the responses are shown in table 5 and figs. 13–16.

Comment: In the first time, when increasing the value of static load P_d, the vertical displacement at the top of the system is changed faster than the horizontal displacement. When static load P_d is strong enough, horizontal displacement at the top of the truss increases suddenly. The computer program is stopped because the non-convergence leads to the unstable structure. We determine the critical value of the system with the given set of parameters $P_d = 2.8\times10^8$ N corresponding to the case $P_0 = 1\times10^6$ N.

Table 5. Displacement response and acceleration at the top of the bar system according to the P_d

P_d (N)	u_{max} (m)	w_{max} (m)	$\ddot{u}_{max}$ (m/s^2)	$\ddot{w}_{max}$ (m/s^2)
1×10^6	0.0984	0.00469	11.,399	1.885
1×10^7	0.1013	0.0135	11.4491	22.376
1×10^8	0.1504	0.1345	13.5499	230.996
2.8×10^8	2.2248	0.6122	243.421	615.297

CONCLUSIONS

In this study, the authors achieve some critical results: Establishing the theoretical foundations and setting up the program to evaluate the dynamic stability of the 3D beam model on the coral foundation; conducting the survey and evaluating the effect of impulse load and static load on the system.

The calculation results above show that when the static load $P_d = 10^6$ N, the system will be unstable when impulse amplitude $P_0 \geq 1.8\times10^7$ N, whereas when impulse amplitude $P_0 = 10^6$ N, the system will be unstable when static load $P_d = 2.8\times10^8$ N.

Data availability: The data used to support the findings of this study are available from the corresponding author upon request.

Conflicts of interest: The authors declare that there are no conflicts of interest regarding the publication of this paper.

Acknowledgments: This research was supported by Le Quy Don University.

REFERENCES

[1] Chung, N. T., Luong, H. X., and Dat, P. T., 2006. Study of interaction between pile and coral foundation. In *National Conference of Engineering Mechanics and Automation, Vietnam National University Publishers, Hanoi* (pp. 35–44).

[2] Hoang Xuan Luong, Pham Tien Dat, Nguyen Thai Chung and Le Tan, 2008. Calculating Dynamic Interaction between the Pipe and the Coral Foundation. *The International Conference on Computational Solid Mechanics, Ho Chi Minh city, Vietnam*, pp. 277–286. (in Vietnamese).

[3] Mahmood, M. N., Ahmed, S. Y., 2006. Nonlinear dynamic analysis of reinforced concrete framed structures including soil-structure interaction effects. *Tikrit Journal of Eng. Sciences*, *13*(3), 1–33.

[4] Ismail, A., 2014. Effect of soil flexibility on seismic performance of 3-D frames. *Journal of Mechanical and Civil Engineering*, *11*(4), 135–143.

[5] Hoang Xuan Luong, 2010. Recapitulative report of the subject No. KC.09.07/06–10. *Le Quy Don University, Vietnam*. (in Vietnamese).

[6] Nguyen Thai Chung, 2015. Recapitulative report of the subject No. KC.09.26/11–15. *Le Quy Don University, Vietnam*. (in Vietnamese).

[7] Graham, N. A. J., and Nash, K. L., 2013. The importance of structural complexity in coral reef ecosystems. *Coral reefs*, *32*(2), 315–326. DOI 10.1007/s00338-012-0984-y.

[8] Nguyen Tien Khiem, Nguyen Thai Chung, Hoang Xuan Luong, Pham Tien Dat, Tran Thanh Hai, 2018. Interaction between structures and sea environment. *Publishing House for Science and Technology*, ISBN: 978-604-913-785-3. (in Vietnamese).

[9] Hoang Xuan Luong, Nguyen Thai Chung, Tran Nghi, Pham Tien Dat, 2016. Coral of Spratly islands - Interaction Between Structures and Coral Foundation. *Construction Publishing House*, IBSN: 978-604-82-1830-0. (in Vietnamese).

[10] Bathe, K. J., and Wilson, E. L., 1976. Numerical methods in finite element analysis (No. BOOK). *Prentice-Hall*.

[11] Wolf, J., and Hall, W., 1988. Soil-structure-interaction analysis in time domain (No. BOOK). *A Division of Simon & Schuster*.

[12] Bathe, K. J., and Wilson, E. L., 1982. Numerical methods in finite element analysis, Transl. from Eng., 448 p. *Strojizdat, Moscow*.

[13] Zienkiewicz, O. C., and Taylor, R. L., 1991. The finite element method. Vol. 2: solid and fluid mechanics, dynamics and non-linearity.

[14] Walker, A. C., Ellinas, C. P., and Supple, W. J., 1984. Buckling of offshore structures. *Gulf Publishing Company*.

[15] Hidalgo, E. M., 2014. Study of optimization for vibration absorbing devices applied on airplane structural elements. *Doctoral dissertation, Universitat Politècnica de Catalunya. Escola Tècnica Superior d'Enginyeries Industrial i Aeronàutica de Terrassa. Departament de Projectes d'Enginyeria, 2014 (Grau en Enginyeria en Tecnologies Aeroespacials)*.

[16] Tzamtzis, A. D., and Asteris, P. G., 2004. FE analysis of complex discontinuous and jointed structural systems (Part 1: Presentation of the method-a state-of-the-art review). *Electronic Journal of Structural Engineering*, *1*, 75–92.

[17] Dynamic analysis of Jacket type offshore structure under impact of wave and wind using Stoke's second order wave theory. *Vietnam Journal of Marine Science and Technology*, *15*(2), 200–208. https://doi.org/10.15625/1859-3097/15/2/6507.

Appendix

A.1. The linear stiffness matrix $[K]_b^e$ is:

$$[K]_b^e = \begin{bmatrix} [K_{11}] & [K_{12}] \\ [K_{21}] & [K_{22}] \end{bmatrix},$$

$$[K_{ii}] = \begin{bmatrix} \frac{EA}{l_e} & 0 & 0 & 0 & 0 & 0 \\ 0 & \frac{12EJ_z}{l_e^3} & 0 & 0 & 0 & \varsigma_i \frac{6EJ_z}{l_e^2} \\ 0 & 0 & \frac{EJ_y}{l_e^3} & 0 & -\varsigma_i \frac{6EJ_y}{l_e^2} & 0 \\ 0 & 0 & 0 & \frac{GJ_p}{l_e} & 0 & 0 \\ 0 & 0 & -\varsigma_i \frac{6EJ_y}{l_e^2} & 0 & \frac{4EJ_y}{l_e} & 0 \\ 0 & \varsigma_i \frac{6EJ_z}{l_e^2} & 0 & 0 & 0 & \frac{4EJ_z}{l_e} \end{bmatrix}, i = \overline{1,2}, \varsigma_1 = 1, \varsigma_2 = -1$$

$$[K_{21}]=\begin{bmatrix} -\frac{EA}{l_e} & 0 & 0 & 0 & 0 & 0 \\ 0 & -\frac{12EJ_z}{l_e^3} & 0 & 0 & 0 & -\frac{6EJ_z}{l_e^2} \\ 0 & 0 & -\frac{12EJ_y}{l_e^3} & 0 & \frac{6EJ_y}{l_e^2} & 0 \\ 0 & 0 & 0 & -\frac{GJ_p}{l_e} & 0 & 0 \\ 0 & 0 & -\frac{6EJ_y}{l_e^2} & 0 & \frac{2EJ_y}{l_e} & 0 \\ 0 & \frac{6EJ_z}{l_e^2} & 0 & 0 & 0 & \frac{2EJ_z}{l_e} \end{bmatrix}, [K_{12}]=[K_{21}]^T$$

A.2. The non-linear stiffness matrix $\left[K_G\right]_e^b$ is:

$$[K_G]_b^e=\frac{N_x}{30l_e}\begin{bmatrix} 0 & 0 & 0 & 0 & 0 & 0 & 0 & 0 & 0 & 0 & 0 & 0 \\ 0 & 36 & 0 & 0 & 0 & 3l_e & 0 & -36 & 0 & 0 & 0 & 3l_e \\ 0 & 36 & 0 & 0 & 3l_e & 0 & 0 & 0 & -36 & 0 & 3l_e & 0 \\ 0 & 0 & 0 & 0 & 0 & 0 & 0 & 0 & 0 & 0 & 0 & 0 \\ 0 & 0 & 3l_e & 0 & 4l_e^2 & 0 & 0 & 0 & -3l_e & 0 & l_e^2 & 0 \\ 0 & 3l_e & 0 & 0 & 0 & 4l_e^2 & 0 & -3l_e & 0 & 0 & 0 & l_e^2 \\ 0 & 0 & 0 & 0 & 0 & 0 & 0 & 0 & 0 & 0 & 0 & 0 \\ 0 & -36 & 0 & 0 & 0 & -3l_e & 0 & 36 & 0 & 0 & 0 & -3l_e \\ 0 & 0 & -36 & 0 & -3l_e & 0 & 0 & 0 & 36 & 0 & -3l_e & 0 \\ 0 & 0 & 0 & 0 & 0 & 0 & 0 & 0 & 0 & 0 & 0 & 0 \\ 0 & 0 & 3l_e & 0 & l_e^2 & 0 & 0 & 0 & -3l_e & 0 & 4l_e^2 & 0 \\ 0 & 3l_e & 0 & 0 & 0 & l_e^2 & 0 & -3l_e & 0 & 0 & 0 & 4l_e^2 \end{bmatrix}$$

Where: N_x is the axial force of beam element; J_p is the torsional constant; J_y and J_z respectively are the moments of inertia about the *y* and *z* axes of the element.

A.3. The mass matrix $\left[M\right]_e^b$ is

$$[M]_b^e=\begin{bmatrix} [M_{11}] & [M_{12}] \\ [M_{21}] & [M_{22}] \end{bmatrix}, [M_{11}]=\rho Al_e\begin{bmatrix} \frac{1}{3} & 0 & 0 & 0 & 0 & 0 \\ 0 & \frac{13}{35} & 0 & 0 & 0 & \frac{11l_e}{210} \\ 0 & 0 & \frac{13}{35} & 0 & -\frac{11l_e}{210} & 0 \\ 0 & 0 & 0 & \frac{J_y+J_z}{3A} & 0 & 0 \\ 0 & 0 & -\frac{11l_e}{210} & 0 & \frac{l_e^2}{105} & 0 \\ 0 & \frac{11l_e}{210} & 0 & 0 & 0 & \frac{l_e^2}{105} \end{bmatrix},$$

$$[M_{12}]=\rho A l_e\begin{bmatrix}\frac{1}{6} & 0 & 0 & 0 & 0 & 0\\ 0 & \frac{9}{70} & 0 & 0 & 0 & -\frac{13l_e}{420}\\ 0 & 0 & \frac{9}{70} & 0 & -\frac{13l_e}{420} & 0\\ 0 & 0 & 0 & \frac{J_y+J_z}{6A} & 0 & 0\\ 0 & 0 & -\frac{13l_e}{420} & 0 & -\frac{l_e^2}{140} & 0\\ 0 & \frac{13l_e}{420} & 0 & 0 & 0 & -\frac{l_e^2}{140}\end{bmatrix},$$

$$[M_{21}]=\rho A l_e\begin{bmatrix}\frac{1}{6} & 0 & 0 & 0 & 0 & 0\\ 0 & \frac{9}{70} & 0 & 0 & 0 & \frac{13l_e}{420}\\ 0 & 0 & \frac{9}{70} & 0 & -\frac{13l_e}{420} & 0\\ 0 & 0 & 0 & \frac{J_y+J_z}{6A} & 0 & 0\\ 0 & 0 & \frac{13l_e}{420} & 0 & -\frac{l_e^2}{140} & 0\\ 0 & -\frac{13l_e}{420} & 0 & 0 & 0 & -\frac{l_e^2}{140}\end{bmatrix},$$

$$[M_{22}]=\rho A l_e\begin{bmatrix}\frac{1}{3} & 0 & 0 & 0 & 0 & 0\\ 0 & \frac{13}{35} & 0 & 0 & 0 & -\frac{11l_e}{210}\\ 0 & 0 & \frac{13}{35} & 0 & \frac{11l_e}{210} & 0\\ 0 & 0 & 0 & \frac{J_y+J_z}{3A} & 0 & 0\\ 0 & 0 & \frac{11l_e}{210} & 0 & \frac{l_e^2}{105} & 0\\ 0 & -\frac{11l_e}{210} & 0 & 0 & 0 & \frac{l_e^2}{105}\end{bmatrix}.$$

ρ is the mass density of beam.